Offset Mismatch Calibration for TI-ADCs in High-Speed OFDM Systems

Vo-Trung-Dung Huynh, Nele Noels, Heidi Steendam

Department of Telecommunications and Information Processing, Ghent University

{votrungdung.huynh, nele.noels, heidi.steendam}@telin.ugent.be

Abstract—Time-interleaved analog-to-digital converters (TI-ADCs) are widely used for multi-Gigabit orthogonal frequency division multiplexing (OFDM) based systems because of their attractive high sampling rate and high resolution. However, when not perfectly calibrated, mismatches such as offset mismatch, gain mismatch and timing mismatch between parallel sub-ADCs can significantly degrade the system performance. In this paper, we focus on offset mismatch. We analyze two calibration techniques for the offset mismatch, based on the least-squares (LS) and linear minimum mean-squared error (LMMSE) algorithms assuming an AWGN channel. The simulation results show that our method is capable of improving the BER performance. As expected, the LMMSE estimator outperforms the LS estimator. However, at large offset mismatch levels or low noise level, both estimators converge. In this paper, we derive the condition on the mismatch level for convergence between the two estimators.

Index Terms—OFDM, TI-ADC, offset mismatch, least-squares, linear minimum mean-squared error, mean-squared error, calibration.

Fig. 1. Block diagram of a TI-ADC.

I. INTRODUCTION

Orthogonal frequency division multiplexing (OFDM) has recently received increased attention for multi-Gigabit fiber-optic communication systems due to its effectiveness in providing high bandwidth capability and eliminating inter-symbol interference [1]. To allow for the high data rates required for such OFDM systems, an extremely high-sampling-rate analog-to-digital converter (ADC), placed in front of the baseband digital signal processing (DSP) unit, is required. However, such high-sampling-rate ADCs are not fabricated because of the physical constraints of the current technology [2]. A low cost alternative to these hardware restrictions is the time-interleaved ADC (TI-ADC), which is shown in Fig. 1 [3]. The lth parallel lower sampling-rate ADC slicer of a TI-ADC samples the signal at instants CK_l, $l = 0, 1, ..., L − 1$, where L is the number of sub-ADCs, and the sampling instants are equidistantly shifted in time with as spacing the ideal sampling time T_s. In this way, the overall sampling rate of the TI-ADC is L times larger than the sampling rate $\frac{1}{LT_s}$ of each sub-ADC. However, mismatches between the sub-ADCs in a TI-ADC degrade the system performance if not calibrated. One of the major mismatches is offset mismatch, which is caused by the differences in the comparators' input-referred offsets [4]. Without calibration, offset mismatch can cause an error floor in the bit error rate (BER) performance of the OFDM system [5]. In [6], the authors introduced an objective function to estimate the offset mismatch and then eliminate its effect in the digital domain. However, their approach needs a large number of OFDM symbols. In [7], the decorrelation least-mean-square (LMS) algorithm and the recursive-least-square (RLS) algorithm were proposed to calibrate the offset mismatch. However, these techniques require the presence of comb-type pilot tones in the OFDM signal. In this paper, we propose two simple offset-mismatch calibration methods based on the least-squares (LS) and the linear minimum mean-square-error (LMMSE) principles, using less OFDM symbols than [6], without employing pilot tones. The effectiveness of our proposed methods is confirmed by simulation results in terms of the BER performance. We show that the LS estimator is able to remove the offset mismatch and the corresponding error floor in the BER performance. However, the LS estimator comes with a 3 dB penalty in the BER performance because of the noise enhancement. The more complex LMMSE estimator, on the other hand, suffers less from noise enhancement, although the LMMSE estimator converges to the LS estimator for low noise level or high offset mismatch levels. In this paper, we investigate the threshold levels for the noise and the offset mismatch at which both estimators converge.

The paper is organized as follows. In Section II, we describe the model of an OFDM system employing a TI-ADC suffering from offset mismatch. An analysis of the proposed methods is given in Section III. In section IV, we validate the capability of the proposed calibration methods by simulation, and we also derive the threshold for the offset mismatch level, causing convergence of the LS and LMMSE estimator. Finally, our conclusion is given in Section V.
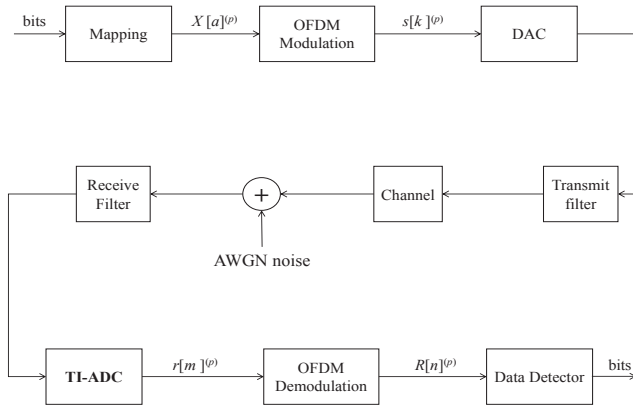
Fig. 2. Block diagram of an OFDM system with a TI-ADC at receiver.

II. System Model

Fig. 2 shows a block diagram of an OFDM system employing a TI-ADC at the receiver. Let us define the vector $\mathbf{\Lambda}$, which consists of P blocks $\mathbf{X}^{(p)}$, $p = 0, 1, ..., P - 1$, as the input of the inverse discrete Fourier transform (IDFT). Each block $\mathbf{X}^{(p)}$ contains N complex-valued symbols, i.e., $\mathbf{X}^{(p)} = \left(X\left[-\frac{N}{2}\right]^{(p)}, X\left[-\frac{N}{2} + 1\right]^{(p)}, ..., X\left[\frac{N}{2} - 1\right]^{(p)} \right)^{T}$, where the superscript T denotes transpose, which are taken from an M-ary phase shift keying (PSK) or quadrature amplitude modulation (QAM) constellation. The IDFT unit converts the frequency-domain blocks $\mathbf{X}^{(p)}$ to the time-domain samples $s[k]^{(p)}$, given by[1]:

$$s[k]^{(p)} = \frac{1}{\sqrt{N}} \sum_{a=-\frac{N}{2}}^{\frac{N}{2}-1} X[a]^{(p)} e^{-j2\pi \frac{ak}{N}},$$
$$k = -\frac{N}{2}, -\frac{N}{2} + 1, ..., \frac{N}{2} - 1, \ p = 0, 1, ..., P - 1. \quad (1)$$

Before transmission through the channel, the time-domain samples are converted to an analog signal by a digital-to-analog converter (DAC) and a transmit filter is used to eliminate the transmitted signal's images produced by the DAC. As we want to focus on offset mismatch calibration, we assume an AWGN channel, and the transmit and receive filters are matched.

After passing the receive filter, the received waveform is sampled at Nyquist rate by a TI-ADC consisting of L parallel sub-ADCs. The TI-ADC is assumed to have sufficiently high resolution such that the quantization noise can be neglected [8]. Assuming the TI-ADC is affected by offset mismatch only and using the model of a TI-ADC introduced in [9], the output of the TI-ADC can be written as:

$$r[m]^{(p)} = s[k]^{(p)} + do_{(m+Np)|L} + w[m]^{(p)},$$
$$, m = -\frac{N}{2}, -\frac{N}{2} + 1, ..., \frac{N}{2} - 1, \quad (2)$$

where $r[m]^{(p)}$ denotes the mth sample of the pth OFDM block, $do_{(m+Np)|L}$ is the offset of the sub-ADC, $x|y$ denotes

the modulo operation of x with respect to y, and $w[m]^{(p)}$ is the AWGN noise sample with zero mean and variance $\sigma_w^2 = \frac{N_0}{2}$ per in-phase/quadrature dimension, with N_0 the noise power spectral density. The received samples are then applied to the DFT unit. In order to analyze our calibration approach, we write the output of the DFT unit of the pth OFDM block as:

$$\mathbf{R}_{DFT}^{(p)} = \mathbf{X}^{(p)} + \mathbf{F}\mathbf{e}^{(p)} + \mathbf{W}^{(p)}, \quad (3)$$

where $\mathbf{X}^{(p)}$ is the vector of the transmitted symbols, $\mathbf{W}^{(p)}$ is the AWGN noise vector in frequency domain, $\mathbf{e}^{(p)}$ is the offset mismatch vector given by:

$$\left(\mathbf{e}^{(p)}\right)_m = do_{(m+Np)|L} \ , m = -\frac{N}{2}, -\frac{N}{2} + 1, ..., \frac{N}{2} - 1, \quad (4)$$

and $\mathbf{F}$ is the $N \times N$ DFT matrix defined as:

$$(\mathbf{F})_{n,m} = \frac{1}{\sqrt{N}} e^{-j2\pi \frac{nm}{N}},$$
$$n, m = -\frac{N}{2}, -\frac{N}{2} + 1, ..., \frac{N}{2} - 1. \quad (5)$$

In the next section, we will analyze the proposed calibration methods to estimate the offset mismatch vector $\mathbf{e}^{(p)}$ and compensate the offset mismatch error in the frequency domain.

III. Offset Mismatch Calibration

In the following, we assume the ratio $\frac{N}{L}$ between the IDFT/DFT size and the number of sub-ADCs is an integer value. It is shown in [5] that when the DFT/IDFT size N is a multiple of the number L of sub-ADCs, the offset mismatch error only has an effect on the sub-carriers with index equal to a multiple of $\frac{N}{L}$, while the other sub-carriers are not affected[2]. In that case, the contribution from the offset mismatch, i.e., $do_{(m+Np)|L}$ and $\mathbf{e}^{(p)}$, becomes independent of the block index p. Hence, the number of affected sub-carriers per OFDM block equals the number L of sub-ADCs. Fig. 3 illustrates the block diagram of the proposed calibration technique. The first OFDM symbol is used as a preamble in which no data is transmitted at the sub-carriers with indices $i\frac{N}{L}$, $i = -\frac{L}{2}, -\frac{L}{2} + 1, ..., \frac{L}{2} - 1$, i.e., the affected sub-carriers. Extracting those sub-carriers at the output of the DFT in the first OFDM symbol, we obtain the offset mismatch vector $\mathbf{E}^{(0)}$ in the frequency domain:

$$\mathbf{E}^{(0)} = \mathbf{F}_1 \mathbf{e}_1 + \mathbf{W}_1^{(0)}, \quad (6)$$

where the superscript (0) denotes the first OFDM symbol, $\left(\mathbf{E}^{(0)}\right)_i = \left(\mathbf{R}_{DFT}^{(0)}\right)_{\frac{iN}{L}}$, $\mathbf{W}_1^{(0)}$ is the AWGN noise vector, $\mathbf{e}_1$ is the offset vector defined as:

$$(\mathbf{e}_1)_l = do_l, \qquad l = 0, 1, ..., L - 1, \quad (7)$$

and $\mathbf{F}_1$ is a $L \times L$ matrix given by:

$$(\mathbf{F}_1)_{i,l} = \frac{\sqrt{N}}{L} e^{-j2\pi \frac{il}{L}},$$
$$i = -\frac{L}{2}, -\frac{L}{2} + 1, ..., \frac{L}{2} - 1, \ l = 0, 1, ..., L - 1. \quad (8)$$

The estimate $\hat{\mathbf{E}}$ of $\mathbf{F}_1 \mathbf{e}_1$ is saved in the register, and is used to compensate the first OFDM symbol and the following

---

[1]In practice, a guard interval is inserted in the time-domain to counteract the effect of the dispersive channel. However, as an AWGN channel is considered in this paper, we omit the guard interval.

[2]When the ratio $\frac{N}{L}$ is not an integer value, all sub-carriers are affected by the offset mismatch.
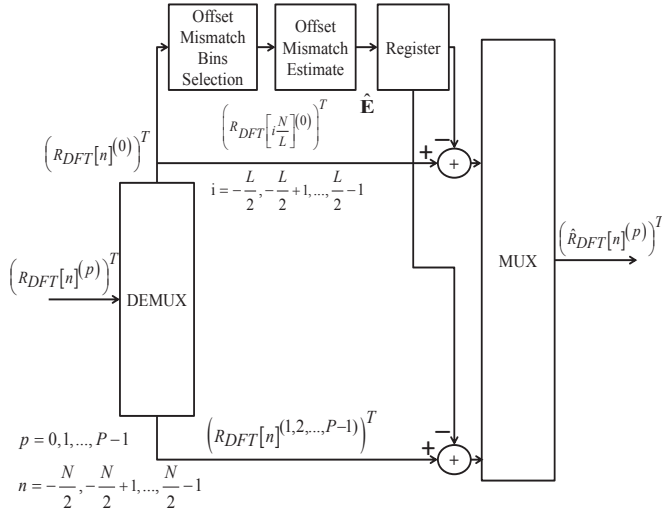
Fig. 3. Block diagram of the proposed calibration approach.

OFDM symbols by subtraction in the frequency domain, as shown in Fig. 3. Hence, in order to estimate the contribution from the offset mismatch, we use only one OFDM symbol. In the following, we consider the LS and LMMSE approaches to obtain the estimate $\hat{\mathbf{E}}$.

• **Least-Squares Estimation**: The LS estimate $\hat{\mathbf{E}}_{LS}$ of of $\mathbf{F}_1\mathbf{e}_1$ equals [10]:

$$\hat{\mathbf{E}}_{LS} = \mathbf{E}^{(0)}. \tag{9}$$

The mean-square error (MSE) of the LS estimate equals

$$MSE_{LS} = E\left\{\left\|\mathbf{F}_1\mathbf{e}_1 - \hat{\mathbf{E}}_{LS}\right\|^2\right\} = \sigma_w^2, \tag{10}$$

where $E\{.\}$ denotes averaging over the noise distribution. Taking into account that the noise samples $\mathbf{W}_1^{(0)}[l]$ on the different sub-carriers are independent and have the same variance σ_w^2, the estimate $\hat{\mathbf{E}}_{LS}[l]$ will be gaussian distributed with variance σ_w^2, which is independent of the sub-carrier index. As a result, in the successive OFDM blocks, the calibration removes the offset mismatch contribution on the affected sub-carriers, but at the same time adds an additional AWGN term with variance σ_w^2 to the sub-carriers with indices $i\frac{N}{L}$, i.e., $\mathbf{R}_{DFT_{comp}, i\frac{N}{L}}^{(p)} = \mathbf{X}_{i\frac{N}{L}}^{(p)} + \mathbf{W}_{1,i\frac{N}{L}}^{(p)} - \mathbf{W}_{1,i\frac{N}{L}}^{(0)}$, implying the noise level will be doubled. Consequently, we expect that, although the effect of the offset mismatch is compensated for, the BER of the affected sub-carriers will suffer from a 3 dB loss in terms of the SNR.

• **Linear Minimum Mean-Squared-Error Estimation**: To reduce the 3 dB loss introduced by the noise enhancement in the LS estimator, the LMMSE estimator uses a weight matrix such that the MSE is minimized. As a result, the LMMSE estimate is given by [10]:

$$\hat{\mathbf{E}}_{LMMSE} = \mathbf{R}\left(\mathbf{R} + \sigma_w^2\mathbf{I}\right)^{-1}\mathbf{E}^{(0)}, \tag{11}$$

where $\mathbf{R}$ is the auto-correlation matrix of $\mathbf{F}_1\mathbf{e}_1$, i.e., $\mathbf{R} = E\left\{\mathbf{F}_1\mathbf{e}_1\mathbf{e}_1^H\mathbf{F}_1^H\right\}$, and $\mathbf{I}$ is the identity matrix. The MSE of

the LMMSE estimate equals:

$$
\begin{aligned}
MSE_{LMMSE} &= E\left\{\left\|\mathbf{F}_1\mathbf{e}_1 - \hat{\mathbf{E}}_{LMMSE}\right\|^2\right\} \\
&= \tfrac{1}{L}Trace\left\{\mathbf{R}\left(\mathbf{I} - \left(\mathbf{R} + \sigma_w^2\mathbf{I}\right)^{-1}\mathbf{R}\right)\right\}, \\
&= \tfrac{\sigma_w^2}{L}\sum_{l=0}^{L-1}\frac{\lambda_l}{\lambda_l + \sigma_w^2}
\end{aligned}
\tag{12}
$$

where λ_l are the eigenvalues of the auto-correlation matrix $\mathbf{R}$. As $\mathbf{R}$ is a positive (semi-) definite matrix, $\lambda_l \geq 0$. Taking into account that $\sum_{l=0}^{L-1} \lambda_l = Trace\{\mathbf{R}\} = \sum_{l=0}^{L-1} E\left\{|\mathbf{e}_1[l]|^2\right\} = \sum_{l=0}^{L-1} E\left\{|do_l|^2\right\}$, it follows that the magnitude of the eigenvalues depends on the level of the offset mismatch. When the level of the offset mismatch is small, i.e., when $\lambda_l \ll \sigma_w^2$, the MSE in (12) can be approximated by $MSE_{LMMSE} \approx \frac{1}{L}\sum_{l=0}^{L-1}\lambda_l \approx \frac{1}{L}\sum_{l=0}^{L-1} E\left\{|do_l|^2\right\} \ll MSE_{LS}$. Hence, the LMMSE estimator will outperform the LS estimator. Similarly, when the offset mismatch level is large, i.e., when $\lambda_l \gg \sigma_w^2$, the MSE in (12) is approximated by $MSE_{LMMSE} \approx \sigma_w^2 = MSE_{LS}$, i.e., the LMMSE estimator converges to the LS estimator for large values of the offset mismatch or low values of the noise level.

IV. NUMERICAL RESULTS

In this section, we validate our proposed methods in terms of the MSE performance and the BER performance. The parameters for the simulations are summarized in Table I. The offset values are uniformly chosen in the interval $\left[-\alpha\sqrt{E_s}, \alpha\sqrt{E_s}\right]$, where E_s is the transmitted energy of a data symbol, and α is the level of the offset mismatch. In this paper, we express the level of the offset mismatch in percentage, i.e., $\alpha\% = \frac{\alpha}{100}$, with respect to the amplitude level $\sqrt{E_s}$, and the signal-to-noise ratio SNR is defined as SNR $= \frac{E_b}{N_0} = \frac{E_b}{2\sigma_w^2}$, where $E_b = \frac{E_s}{\log_2 M}$.

TABLE I
SIMULATION PARAMETERS

Parameters	Reference values
FFT size	2048
Data carriers	1705
Modulation (M-QAM)	16-QAM
Number of sub-ADCs	8

First, to examine the efficiency of the proposed calibration methods, we observe the scatter diagram at the receiver without offset mismatch and with 10% mismatch, and the scatter diagram before and after offset mismatch compensation using the LS and LMMSE estimators for SNR = 17 dB. From Fig. 4, it can be seen that without calibration, the offset mismatch causes data-independent points in the scatter diagram, while these data-independent points have vanished after compensation, for both the LS and LMMSE estimators. Hence, we expect that the proposed calibration methods are able to dissolve the error floor caused by the offset mismatch in the BER performance. Further, we observe that, as expected,
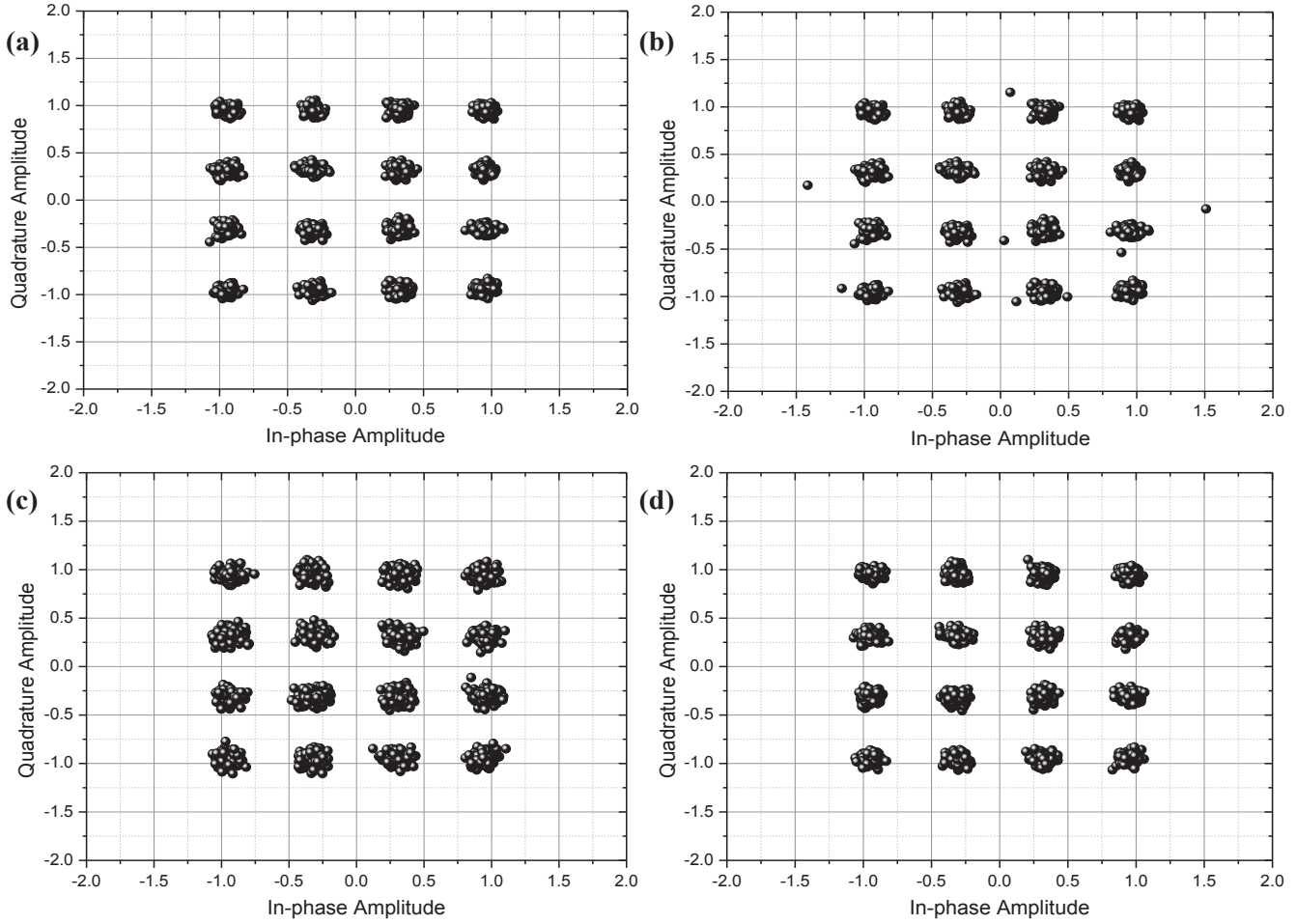
Fig. 4. Scatter diagram for 16-QAM at SNR = 17 dB: (a) Without mismatch. (b) 10% mismatch, (c) After compensation: LS estimator-10% mismatch, (d) After compensation: LMMSE estimator-10% mismatch.

the size of the clouds around the constellation points after compensation is larger for the LS estimator, as the noise level is doubled as compared to the case without offset mismatch. The size of the clouds in the case of the LMMSE estimator is smaller and comparable to the "no mismatch" case.

Next, we consider the MSE performance of the LS and LMMSE estimators. As expected, the MSE of the LS estimator is constant, i.e., MSE = σ_w^2, while the MSE of the LMMSE estimator increases as a function of the mismatch level α, and converges to that of the LS estimator. The level α at which both estimators converge, reduces when the noise level σ_w^2 reduces, or when the energy per symbol E_s increases. This can be explained as follows. The eigenvalues λ_l of the auto-correlation matrix $\mathbf{R}$ are proportional to $\alpha^2 E_s$, as $\sum_{l=0}^{L-1} \lambda_l = \sum_{l=0}^{L-1} E\left\{|do_l|^2\right\} = \frac{L\alpha^2 E_s}{3}$. In the previous section, we have shown that, when $\lambda_l \gg \sigma_w^2$, the LMMSE estimator converges to the LS estimator. Let us define $\gamma\sigma_w^2$ as the threshold level at which convergence occurs, with $\gamma \gg 1$. Hence, when $\sum_{l=0}^{L-1} \lambda_l = \frac{L\alpha^2 E_s}{3} \gg L\gamma\sigma_w^2$, the LMMSE estimator will have the same performance as the LS estimator.

Rewriting this inequality, we obtain:

$$\gamma \leq \frac{\alpha^2 E_s}{3\sigma_w^2} = \frac{2}{3}\alpha^2 \cdot SNR \cdot \log_2 M. \qquad (13)$$

Inspecting Fig. 5, we find that $\gamma = 100$ will result in converge. From the inequality (13), we obtain a threshold on the noise level, for given mismatch level α, or a threshold on the mismatch level α, for given noise level or SNR level. Further, (13) illustrates that, when $SNR \geq \frac{150}{\alpha^2 \cdot \log_2 M}$, the LMMSE estimator will be close to the LS estimator in terms of the BER performance.

Fig. 6 presents the ideal, un-calibrated and calibrated BER curves for 10% and 100% mismatch. When the offset mismatch is not compensated, we see it causes an error floor in the BER performance. Both the LS estimator and the LMMSE estimator are able to eliminate this error floor for all cases. Moreover, as expected, the LS estimator causes a 3 dB loss in the BER performance. Further, from (13), we can expect that the BER of the LMMSE estimator is close to that of the LS estimator for SNR $\geq$ 15.74 dB for 100% mismatch. This threshold can be observed in the figure. In the 10% mismatch case, it follows from (13) that convergence between the two estimators will occur when SNR $\geq$ 35.74 dB. As the
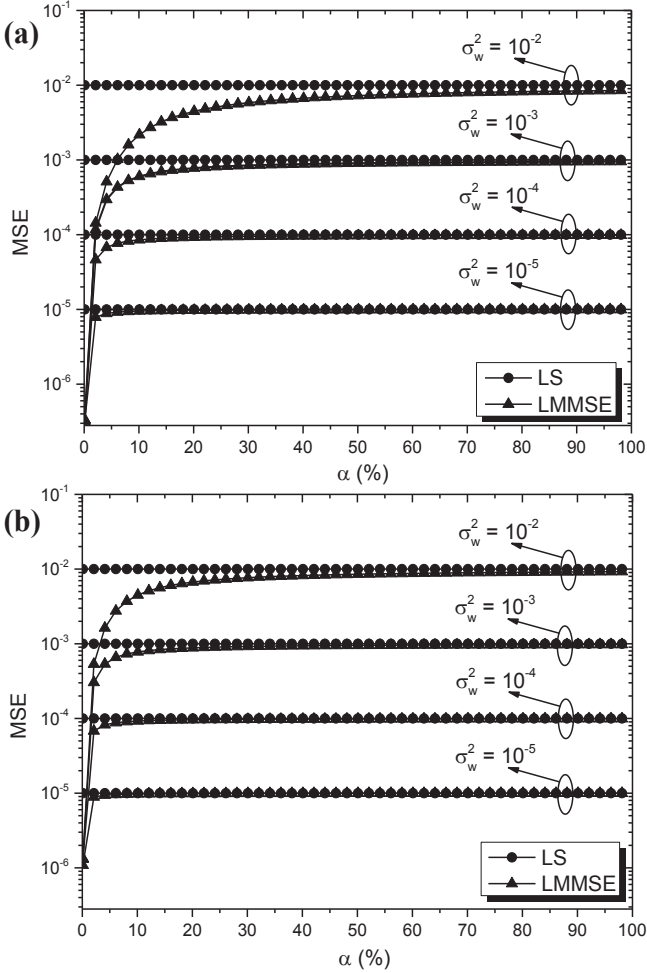
Fig. 5. MSE performance of the LS estimator and the LMMSE estimator: (a) $E_s = 1$, (b) $E_s = 2$.

corresponding BER is very small at this SNR, it follows that for practical situations, the LMMSE estimator will outperform the LS estimator for low to moderate mismatch levels. Hence, (13) is useful in predicting the performance of the LMMSE estimator. When the SNR is larger than this threshold, the LS estimator is preferred, as it has a lower complexity than the LMMSE estimator. However, below this threshold, the LMMSE estimator is selected as it has a better performance.
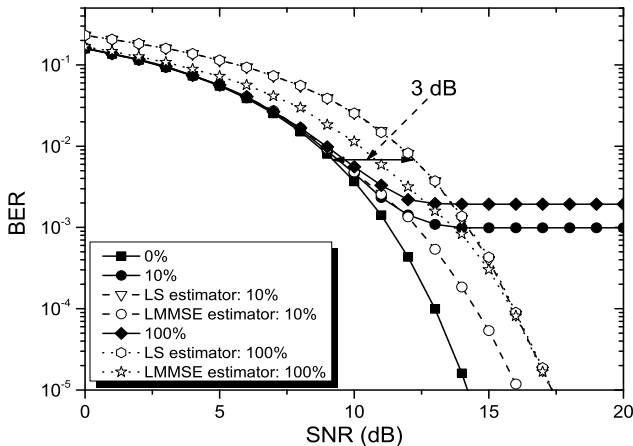
V. CONCLUSIONS

In this paper, we proposed two simple offset-mismatch calibration methods for a TI-ADC, based on the LS and LMMSE approaches, in a high-speed OFDM system assuming an AWGN channel. Our results show that the proposed methods can completely eliminate the error floor caused by offset mismatch without the need of pilots and only one OFDM symbol is required to estimate the offset mismatch. The LS estimator-based calibration causes a 3 dB BER performance degradation, but the calibration based on the LMMSE estimator is able to improve the BER performance. Although the LMMSE estimator will converge to the LS estimator in terms of the MSE and BER performances for large offset mismatch level values or low noise level, we show in this paper that for low to moderate mismatch levels, the LMMSE estimator gives good results at practical values of the SNR, causing a moderate BER penalty.

ACKNOWLEDGMENT

REFERENCES

[1] J. Armstrong, "OFDM for Optical Communications," *J. Lightwave Technol.,* vol. 27, no. 1, pp. 189-204, Feb. 2009.
[2] W. C. Black and D. A. Hodges, "Time Interleaved Converter Arrays," *IEEE J. Solid-State Circuits,* vol. SSC-15, no. 6, pp. 1022-1029, Dec. 1980.
[3] C. Vogel and H. Johansson, "Time-Interleaved Analog-To-Digital Converters: Status and Future Directions," *Proc. IEEEE Intl. Symp. Circuits Syst.,* May 2006.
[4] S. W. Sin, S. P. U and R. P. Martins, *Generalized Low-Voltage Circuit Techniques for Very High-Speed Time-Interleaved Analog-to-Digital Converters,* Springer, 2011.
[5] V. Huynh, N. Noels, P. Rombouts, J. Armstrong, and H. Steendam, *Effect of Time-Interleaved Analog-to-Digital Converter Mismatches on OFDM Performance,* IEEE Inter. OFDM Workshop, pp. 128-135, Aug. 2014.
[6] Y. Oh, and B. Murmann, *System Embedded ADC Calibration for OFDM Receivers,* IEEE Trans. on Circuits and Systems, vol. 53, no. 8, Aug. 2006.
[7] Y. Zheng, Z. Yan, J. Ma, and G. He, *DC Offset Mismatch Calibration for Time-Interleaved ADCs in High-Speed OFDM Receivers,* NCCET, CCIS 337, pp. 221-230, 2013
[8] H. Johansson and P. Lowenborg, "Reconstruction of non-uniformly sampled bandlimited signals by means of digital fractional delay filters," *IEEE Trans. Signal Process.,* vol. 50, no. 11, pp. 2757-2767, Nov. 2002.
[9] J. Elbornsson, F. Gustafsson, and J-E. Eklund, *Analysis of Mismatch Effects in a Randomly Interleaved A/D Converter System,* IEEE Trans. on Circuit and Systems, vol. 52, no. 3, 2005.
[10] Y. S. Cho, J. Kim, W. Y. Yang and C. G. Kang, *MIMO-OFDM Wireless Communications with MATLAB,* Wiley-IEEE Press, 1st edition, Nov. 2010.

Fig. 6. The ideal, un-calibrated and calibrated BER curves for 16-QAM.